

# Oxovanadium(V) Alkoxide Derivatives of 1,2-Diols: Synthesis and Solid-State $^{51}\text{V}$ NMR Characterization<sup>†</sup>

Debbie C. Crans,<sup>\*,‡</sup> Robert A. Felty,<sup>‡</sup> Haojiang Chen,<sup>‡</sup> Hellmut Eckert,<sup>\*,§</sup> and Nandini Das<sup>§</sup>

Departments of Chemistry, Colorado State University, Fort Collins, Colorado 80523, and University California, Santa Barbara, California 93106

Received September 1, 1993<sup>®</sup>

A new series of oxovanadium(V) 1,2-diolate compounds have been prepared, characterized, and structurally investigated. The reactions of oxovanadium trialkoxides with *trans*-1,2-cyclohexanediol, ( $\pm$ )-2,3-butanediol, 2*R*,3*R*-butanediol, and ethylene glycol produced yellow solid materials. These materials contain two diols for each vanadium presumably in a dimeric arrangement. Solution-state  $^{51}\text{V}$  NMR spectroscopy reveals the presence of complex association and ligand exchange equilibria, necessitating structural characterizations in the solid state. Since single-crystal X-ray diffraction analysis studies were limited as a result of disorder, the materials were characterized by solid-state  $^{51}\text{V}$  and  $^{13}\text{C}$  NMR spectroscopy. Field-dependent line-shape analysis of static and MAS  $^{51}\text{V}$  solid-state NMR spectra obtained on a series of characterized compounds provide benchmark isotropic and anisotropic chemical shift data. These parameters can be correlated to distinct local vanadium coordination environments. On the basis of this correlation, possible structural models for the new oxovanadium 1,2-diolate derivatives were obtained and confirmed by other spectroscopic methods. Changes in coordination about the vanadium atom have been observed when *trans*-1,2-cyclohexanediol, ( $\pm$ )-2,3-butanediol, or 2*R*,3*R*-butanediol is replaced by ethylene glycol. It appears that the molecular geometry about the vanadium atom is very sensitive to minor perturbations in the ligand.

## Introduction

The geometry and structure of vanadium alkoxides are likely to model the vanadium–surface intermediates that form during the oxidation of organic compounds catalyzed by vanadium oxide-based catalysts.<sup>1</sup> In general, the structure of the catalyst during the oxidation reaction is not well understood, although rational catalyst design has been of interest for some time.<sup>1</sup> During homogeneous catalysis, various derivatives are formed using vanadium-based reagents such as  $\text{VO}(\text{acac})_2$  and  $\text{VO}(\text{OR})_n\text{Cl}_{3-n}$  (where  $n = 0, 1, 2,$  and  $3$ ).<sup>2</sup> The nature and geometries of the vanadium complexes that form during reactions are governed by the coordination chemistry and the conformational preferences of the organic ligands. Several recent examples of polyoxovanadium clusters containing alkoxide ligands have been characterized by X-ray crystallography.<sup>3</sup> These examples provide insights into the geometry and chemistry of vanadium alkoxide derivatives.<sup>3–6</sup> Alkoxide bridging,<sup>4</sup> mixed oxide–alkoxide bridging<sup>3</sup> and mixed hydroxide–alkoxide bridging<sup>5</sup> compounds range in size from dimeric materials to clusters containing more than 12 vanadium atoms. The alkoxide ligands coordinate in com-

binations of terminal,  $\mu_2$ , or  $\mu_3$  configurations depending on the alkoxide ligand used and the synthetic procedure implemented. A small number of structural units form the basis for the materials synthesized in organic solvents. In the case of oxovanadium(V) alkoxide derivatives which have alkoxide bridges but no oxide bridges, dinuclear complexes,<sup>4</sup> tetranuclear complexes,<sup>5</sup> and polymeric species<sup>6</sup> have been reported and characterized structurally by X-ray crystallography. However, materials that resist crystallization cannot be characterized in similar detail and convenient methods for structural characterization of these potential catalysts are needed. We describe the use of solid-state  $^{51}\text{V}$  NMR studies for characterization of the coordination number around the vanadium atom in a series of new oxovanadium(V) 1,2-diolates.

Formation of vanadium alkoxides (vanadate esters) in aqueous solutions have been explored using multinuclear NMR and other spectroscopic methods.<sup>7</sup> These compounds form rapidly after mixing vanadate with a variety of alcohols in aqueous solutions.<sup>7b,i</sup> Vanadate monoesters have been found to substitute for phosphate monoesters in enzyme-catalyzed reactions.<sup>8</sup> A recent application of these vanadate esters is the formation of an adenosine 5-phosphate nicotinamide analog (NADP) "NADV" which serves as a good substrate analog for NADP-dependent glucose

<sup>†</sup> This work was funded by the National Institutes of Health (to D.C.C.) and National Science Foundation (to H.E.).

<sup>‡</sup> Colorado State University.

<sup>§</sup> University of California, Santa Barbara.

<sup>®</sup> Abstract published in *Advance ACS Abstracts*, February 15, 1994.

- (1) (a) Whittington, B. I.; Anderson, J. R. *J. Phys. Chem.* **1993**, *97*, 1032. (b) Oyama, S. T.; Somorjai, G. A. *J. Phys. Chem.* **1990**, *94*, 5022. (c) Miyata, H.; Kohno, M.; Ono, T.; Ohno, T.; Hatayama, F. *J. Chem. Soc., Faraday Trans. 1* **1989**, *85*, 3663. (d) Patel, D.; Andersen, P. J.; Kung, H. H. *J. Catal.* **1990**, *125*, 132.
- (2) (a) Trost, B. M.; Fleming, I.; Ley, S. V., Eds. *Comprehensive Organic Synthesis*, Pergamon Press: New York, 1991; Vol. 7, pp 95, 321, 707. (b) Bianchi, M.; Bonchio, M.; Conte, V.; Coppa, F.; Di Furia, F.; Modena, G.; Moro, S.; Standen, S. *J. Mol. Catal.*, in press. (c) Hirao, T.; Mikami, S.; Mori, M.; Oshiro, Y. *Tetrahedron Lett.* **1991**, *32*, 1741. (d) White, J. D.; Butlin, R. J.; Hahn, H.-G.; Johnson, A. T. *J. Am. Chem. Soc.* **1990**, *112*, 8595. (e) Crans, D. C.; Chen, H.; Felty, R. A. *J. Am. Chem. Soc.* **1992**, *114*, 4543 and references therein.
- (3) (a) Chen, Q.; Zubieta, J. *Coord. Chem. Rev.* **1992**, *114*, 107 and references therein. (b) Hou, D.; Hagen, K. S.; Hill, C. L. *J. Am. Chem. Soc.* **1992**, *114*, 5864. (c) Khan, M. I.; Chen, Q.; Goshorn, D. P.; Hope, H.; Parkin, S.; Zubieta, J. *J. Am. Chem. Soc.* **1992**, *114*, 3341. (d) Khan, M. I.; Chen, Q.; Zubieta, J. *Inorg. Chem.* **1990**, *29*, 1458.

- (4) (a) Crans, D. C.; Felty, R. A.; Anderson, O. P.; Miller, M. M. *Inorg. Chem.* **1993**, *32*, 247. (b) Hillerns, F.; Olbrich, F.; Behrens, U.; Rehder, D. *Angew. Chem., Int. Ed. Engl.* **1992**, *31*, 447. (c) Crans, D. C.; Felty, R. A.; Miller, M. M. *J. Am. Chem. Soc.* **1991**, *113*, 265. (d) Preibsch, W.; Rehder, D. *Inorg. Chem.* **1990**, *29*, 3013. (e) Crans, D. C.; Chen, H.; Anderson, O. P.; Miller, M. M. Manuscript in preparation.
- (5) Crans, D. C.; Marshman, R. W.; Gottlieb, M. S.; Anderson, O. P.; Miller, M. M. *Inorg. Chem.* **1992**, *31*, 4939.
- (6) Caughlin, C. N.; Smith, H. M.; Watenpugh, K. *Inorg. Chem.* **1966**, *5*, 2131.
- (7) (a) Tracey, A. S.; Leon-Lai, C. H.; *Inorg. Chem.* **1991**, *30*, 3200. (b) Crans, D. C.; Harnung, S. E.; Larsen, E.; Shin, P. K.; Theisen, L. A.; Trabjerg, I. *Acta Chem. Scand.* **1991**, *45*, 456. (c) Gresser, M. J.; Tracey, A. S.; *J. Am. Chem. Soc.* **1986**, *108*, 1935. (d) Tracey, A. S.; Gresser, M. J.; Galeffi, B. *Inorg. Chem.* **1988**, *27*, 157. (e) Tracey, A. S.; Gresser, M. J. *Inorg. Chem.* **1988**, *27*, 1269. (f) Tracey, A. S.; Galeffi, B.; Mahjour, S. *Can. J. Chem.* **1988**, *66*, 2294. (g) Tracey, A. S.; Gresser, M. J. *Can. J. Chem.* **1988**, *66*, 2570. (h) Gresser, M. J.; Tracey, A. S. *J. Am. Chem. Soc.* **1985**, *107*, 4215. (i) Crans, D. C.; Schelble, S. M.; Theisen, L. A. *J. Org. Chem.* **1991**, *56*, 1266.

6-phosphate dehydrogenase,<sup>8b</sup> 6-phosphogluconate dehydrogenase,<sup>8b</sup> and alcohol dehydrogenase.<sup>8c</sup> The potent interaction of a vanadate-uridine diester inside ribonuclease is well-known.<sup>9</sup> Nevertheless, to date none of these complexes have been characterized by X-ray crystallography although some analogies can be made with the dinuclear oxovanadium alkoxides obtained from organic solvents.<sup>4b-d</sup> The aqueous studies of vanadate and the 1,2-diol ethylene glycol show the formation of a cyclic vanadate-diol complex.<sup>7c,10</sup> Analogous complexes of vanadate with 1,3-diols do not form.<sup>7f,g</sup> Large variations in the distribution of complexes formed in both aqueous and non-aqueous solutions containing vanadate and 1,2-diols or 1,3-diols suggest significant differences in the energetic and/or structural properties of the respective complexes.<sup>5,7c,f,g,10,11</sup> The present paper describes the synthesis and spectroscopic characterization of a series of new oxovanadium(V) 1,2-diolate derivatives.

Many vanadium(V) alkoxides undergo extensive rearrangement and possibly exchange in solution<sup>2e,11,12</sup> so that characterization in both solution and the solid state is essential. Solid-state <sup>51</sup>V NMR spectroscopy has previously provided information on the coordination environment around the vanadium(V) center in vanadium(V) oxide catalysts.<sup>13-15</sup> In this manuscript we describe the first application of solid-state <sup>51</sup>V NMR for structural studies of oxovanadium(V) alkoxides. In addition, other spectroscopic methods are employed to further characterize the materials. A range of structurally well-characterized compounds is used to generate <sup>51</sup>V chemical shift benchmark data which provides the information that allows us to predict the geometry of the vanadium(V) center in a variety of new oxovanadium(V) 1,2-diolates.

## Experimental Section

**Materials and General Procedures.** VO(OCH<sub>3</sub>)<sub>3</sub>,<sup>16</sup> VO(OCH<sub>2</sub>CH<sub>2</sub>-Cl)<sub>3</sub>,<sup>4d</sup> VO(OCH<sub>2</sub>CH<sub>3</sub>)<sub>3</sub>,<sup>17</sup> VO(OCH(CH<sub>3</sub>)<sub>2</sub>)<sub>3</sub>,<sup>18</sup> VO(C(CH<sub>3</sub>)<sub>3</sub>)<sub>3</sub>,<sup>19</sup> VO(O-cyclohexyl)<sub>3</sub>,<sup>19</sup> VO(OCPh<sub>3</sub>)<sub>3</sub>,<sup>2e</sup> VO(O-1-adamantyl)<sub>3</sub>,<sup>2e</sup> VO(O-2-adamantyl)<sub>3</sub>,<sup>2e</sup> VO(O-*exo*-norbornyl)<sub>3</sub>,<sup>2e</sup> VO(O-*endo*-norbornyl)<sub>3</sub>,<sup>2e</sup> VO(O-(*R*)-bornyl)<sub>3</sub>,<sup>2e</sup> VO(O-(*S*)-bornyl)<sub>3</sub>,<sup>2e</sup> (VO)<sub>4</sub>(CH<sub>3</sub>C(CH<sub>2</sub>O)<sub>3</sub>)(OCH<sub>2</sub>CH<sub>3</sub>)<sub>3</sub>,<sup>4e</sup> and (VO)<sub>4</sub>(CH<sub>3</sub>C(CH<sub>2</sub>O)<sub>3</sub>)<sub>2</sub>(OCH<sub>3</sub>)<sub>6</sub><sup>4e</sup> were prepared as previously described. Commercially available starting materials and reagents were reagent quality. Alcohols were dried before use unless stated otherwise. Diol reagents were dried over 3-Å molecular sieves in the case of liquids, or dissolved in methylene chloride and dried over 3-Å molecular sieves in the case of solids. All manipulations were carried out under a nitrogen atmosphere using Schlenk or glovebox techniques. All solvents were dried by standard methods as described by Perrin and Armarego.<sup>20</sup> Yields are reported in millimoles of vanadium atoms.

**General Procedure for Reesterification Reactions of Oxovanadium(V) Trialkoxides with Diols. Reaction between VO(OEt)<sub>3</sub> and *trans*-1,2-Cyclohexanediol To Form 1.** Under an atmosphere of dry nitrogen, dropwise addition of VO(OEt)<sub>3</sub> (0.90 mL, 5.1 mmol) to a toluene

suspension of *trans*-1,2-cyclohexanediol (1.2 grams, 10 mmol) at ambient temperatures produced a cloudy orange solution. After 30 min of stirring, a yellow-orange solid had precipitated from solution. The suspension was stored at -20 °C overnight. The solid was isolated by filtration and weighed 1.3 g (4.4 mmol, 85% yield).

**Specific Procedures. Synthesis. Reaction between VO(OEt)<sub>3</sub> and *trans*-1,2-Cyclohexanediol To Form 1.** The solid yellow product isolated from the reaction of 1.2 g of *trans*-1,2-cyclohexanediol in toluene weighed 1.3 g (4.4 mmol) which corresponds to a 85% yield. The product was characterized as follows. <sup>51</sup>V NMR (78.9 MHz, CH<sub>2</sub>Cl<sub>2</sub>, 298 K): δ -440, -447, -454, -456 ppm. IR (KBr pellet, cm<sup>-1</sup>): 3386 (s), 2936 (2), 2859 (m), 1449 (m), 1397 (w), 1364 (w sh), 1352 (w), 1337 (w), 1329 (vw sh), 1314 (w), 1287 (vw), 1262 (vw), 1232 (w), 1196 (vw), 1181 (w), 1120 (w sh), 1090 (m), 1066 (s), 1046 (s), 979 (m), 957 (m), 929 (m), 883 (w), 857 (m), 790 (w), 737 (w sh), 718 (m), 673 (m), 661 (m), 579 (m), 538 (m), 509 (vw sh), 468 (w), 444 (w), 426 (vw), 402 (w sh), 393 (w). Solid-state <sup>13</sup>C NMR (75.6 MHz, 298 K) δ 97.1, 94.1, 92.1, 76.5, 34.6, 25.5 ppm. Anal. Found (calcd): C, 48.60 (48.65); H, 7.17 (7.15); V, 16.54 (17.20).

**Reaction between VO(OEt)<sub>3</sub> and (±)-2,3-Butanediol To Form 2.** The reaction was performed by using 0.95 g (10 mmol) of (±)-2,3-butanediol in toluene. A bright yellow solid (1.0 g, 4.1 mmol, 81% yield) was isolated by filtration. The product was characterized as follows. <sup>51</sup>V NMR (78.9 MHz, CH<sub>2</sub>Cl<sub>2</sub>, 298 K): δ -455, -466, -473 ppm. IR (KBr pellet, cm<sup>-1</sup>): 3476 (s), 2965 (s), 2929 (m), 2881 (m), 1958 (w), 1437 (m), 1373 (m), 1335 (m), 1311 (m), 1280 (w), 1246 (w), 1141 (m sh), 1126 (m), 1105 (m sh), 1090 (m sh), 1078 (s), 1070 (s), 1056 (s), 989 (s), 982 (s), 939 (m), 924 (s), 894 (m), 823 (m), 690 (s), 683 (s), 674 (s), 661 (s sh), 648 (m sh), 642 (m), 541 (m), 529 (m), 451 (m), 420 (m), 405 (w), 385 (m), 368 (m). Solid-state <sup>13</sup>C NMR (75.6 MHz, 298 K): δ 98.3, 90.1 (double intensity), 73.9, 22.7, 20.3 ppm. Anal. Found (calcd): C, 39.42 (39.55); H, 7.31 (7.02); V, 20.69 (20.86).

**Reaction between VO(OEt)<sub>3</sub> and (2*R*,3*R*)-(-)-2,3-Butanediol To Form 3.** The reaction was performed by using 0.93 g (10 mmol) of (2*R*,3*R*)-(-)-2,3-butanediol in toluene. A bright yellow flaky solid (0.96 g, 3.9 mmol, 77% yield) was isolated by filtration from an orange solution. The product was characterized as follows. <sup>51</sup>V NMR (78.9 MHz, CH<sub>2</sub>Cl<sub>2</sub>, 298 K): δ -482, -487, -490, -499 ppm. IR (KBr pellet, cm<sup>-1</sup>): 3472 (m), 2972 (m), 2930 (w), 2899 (w sh), 2881 (w), 2863 (w sh), 1456 (w sh), 1439 (m), 1374 (m), 1330 (w), 1312 (m), 1282 (w), 1261 (w), 1124 (m sh), 1101 (m sh), 1063 (s), 989 (s), 939 (m), 925 (m), 889 (m), 823 (m), 694 (m), 671 (m sh), 659 (m), 580 (w), 534 (w), 453 (w), 397 (w). Mass spectrum: *m/e* 537 (V<sub>3</sub>C<sub>16</sub>H<sub>32</sub>O<sub>10</sub>), 449, 354, 310, 266, 189. Solid-state <sup>13</sup>C NMR (75.6 MHz, 298 K): δ 99.8, 93.8, 92.3, 90.9, 90.2, 88.3, 73.7 (double intensity), 23.2, 20.6, 19.6 ppm. Anal. Found (calcd): C, 39.55 (39.55); H, 7.12 (7.02); V, 21.09 (20.86).

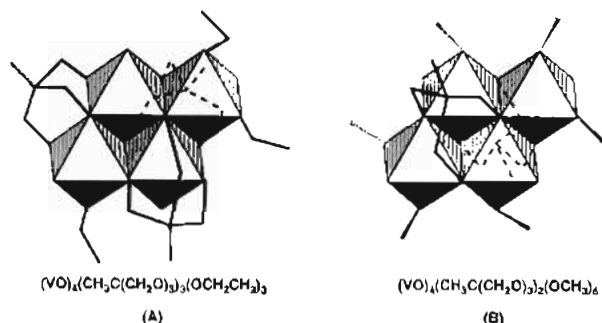
**Reaction between VO(OEt)<sub>3</sub> and Ethylene Glycol To Form 4.** The reaction was performed by using 0.66 g (12 mmol) of ethylene glycol in toluene. A yellow solid (0.79 g, 4.2 mmol, 82% yield) was isolated by filtration from an orange solution. The product was characterized as follows. <sup>51</sup>V NMR (78.9 MHz, CH<sub>2</sub>Cl<sub>2</sub>, 298 K): δ -463, -474, -503, -506, -515. IR (KBr pellet, cm<sup>-1</sup>): 3435 (s), 2971 (w sh), 2948 (m), 2863 (m), 1451 (m sh), 1459 (m), 1380 (m), 1340 (m), 1240 (m), 1212 (m), 1196 (m), 1118 (w), 1071 (s), 1062 (s), 1042 (s), 1024 (m sh), 977 (m), 950 (s), 924 (s), 885 (s), 676 (s), 610 (s), 600 (s), 564 (s), 512 (s). Solid-state <sup>13</sup>C NMR (75.6 MHz, 298 K): δ 83.7 (double intensity), 81.8, 63.7 ppm. Anal. Found (calcd): C, 26.14 (25.55); H, 5.06 (4.82), V, 26.79 (27.09).

**Spectroscopic Methods.** Solution <sup>51</sup>V NMR spectra were recorded at 79.0 MHz on a Bruker ACP-300 NMR spectrometer. <sup>51</sup>V NMR spectra in non-deuterated solvents were recorded with external lock, and chemical shifts were reported against a VOCl<sub>3</sub> reference. Infrared spectra were recorded on a Perkin-Elmer 1600 FT-IR spectrophotometer. Mass spectra were obtained on a VG-MM 16 spectrometer at 453K using EI. Microanalysis was performed by Galbraith Laboratories, Inc., Knoxville, TN.

**Solid-State <sup>51</sup>V NMR Studies.** <sup>51</sup>V solid-state NMR studies were carried out at 79.0 and 131.5 MHz, using General Electric GN-300 and GN-500 spectrometers, equipped with 5- and 7-mm high-speed spinning probes from Doty Scientific. Spinning speeds ranged from 3 to 10 kHz. The spectra were generally recorded with 45° pulses (selective) of 1 μs length and relaxation delays between 1 and 10 s. Complementary static NMR spectra were recorded using a θ-τ-2θ spin echo sequence, with a delay time τ of 50 μs and a relaxation delay of 1 s. In all of the samples studied only the central +1/2 → -1/2 transition of the quadrupolar <sup>51</sup>V nucleus (*I* = 7/2) is being detected. A pulse length θ of 1 μs was chosen,

- (8) (a) Nour-Eldeen, A. F.; Craig, M. M.; Gresser, M. J. *J. Biol. Chem.* **1985**, *260*, 6836. (b) Crans, D. C.; Simone, C. M.; Blanchard, J. S. *J. Am. Chem. Soc.* **1992**, *114*, 4926. (c) Crans, D. C.; Marshman, R. W.; Nielsen, R.; Felty, I. *J. Org. Chem.* **1993**, *58*, 2244.
- (9) Lindquist, R. N.; Lynn, Jr., J. L.; Lienhard, G. E. *J. Am. Chem. Soc.* **1973**, *95*, 8762.
- (10) Ray Jr., W. J.; Zheng, J.; Deng, H.; Burgner, J. W. II. Manuscript in preparation.
- (11) Marshman, R. W.; Crans, D. C.; Chen, H.; Anderson, O. P.; Miller, M. M. Manuscript in preparation.
- (12) Howarth, O. W.; Trainor, J. R. *Inorg. Chim. Acta* **1987**, *127*, L27.
- (13) Eckert, H.; Wachs, I. E. *J. Phys. Chem.* **1989**, *93*, 6796.
- (14) Nabavi, M.; Taulelle, F.; Sanchez, C.; Verdager, M. *J. Phys. Chem. Solids* **1990**, *51*, 1375.
- (15) Sanchez, C.; Nabavi, M.; Taulelle, F. *Mater. Res. Soc. Symp. Proc.* **1990**, *121*, 93.
- (16) Funk, W.; Weiss, W. Z. *Anorg. Allg. Chem.* **1958**, *295*, 327.
- (17) Voronkov, M. G.; Skorik, Iu. I. *Bull. Acad. Sci. USSR, Div. Chem. Soc. (Engl. Transl.)* **1958**, 482.
- (18) Lachowicz, A.; Höbold, W.; Thiele, K.-H.; Z. *Anorg. Allg. Chem.* **1975**, *418*, 65.
- (19) Mittal, R. K.; Mehrotra, R. C. Z. *Anorg. Allg. Chem.* **1964**, *327*, 311.
- (20) Perrin, P. D.; Armarego, W. L. F. *Purification of Laboratory Chemicals*, 3rd ed.; Pergamon Press: New York, 1988.

**Chart 1.** Idealized Polyhedral Models for the Structures  $(VO)_4(CH_3C(CH_2O)_3)_3(OCH_2CH_3)_3$  (A) and  $(VO)_4(CH_3C(CH_2O)_3)_2(OCH_3)_6$  (B)



corresponding to a flip angle of  $45^\circ$  in the selective excitation regime. Variation of  $\theta$  between 1 and 2  $\mu$ s did not affect the results, but with higher pulse lengths, signal distortions due to nonuniform excitation appeared. Appropriate phase cycling was applied in order to cancel out the contribution arising from feedthrough FID signal following the refocusing pulse.<sup>21</sup> Following acquisition, the time domain data was left-shifted to the top of the echo prior to Fourier transformation. All chemical shift values are reported relative to  $VOCl_3$  as an external reference (downfield shifts positive).

**<sup>13</sup>C Solid-State Cross-Polarization-Magic Angle Spinning (CPMAS) NMR Studies.** <sup>13</sup>C solid-state NMR studies were carried out at 75.6 MHz, using a General Electric GN-300 spectrometer. Contact times of 1 ms, recycle delays of 10 s, and spinning speeds around 6 kHz were used. Chemical shifts are reported relative to tetramethylsilane and were determined using a spinning sample of adamantane as an external reference. In certain instances site assignments were aided by interrupted decoupling experiments.

## Results

**Synthesis and Solution Studies of a Series of Known Oxovanadium(V) Trialkoxides.** A series of oxovanadium(V) trialkoxides including  $VO(OCH_3)_3$ ,<sup>16</sup>  $VO(OCH_2CH_2Cl)_3$ ,<sup>4d</sup>  $VO(OCH_2CH_3)_3$ ,<sup>17</sup>  $VO(OCH(CH_3)_2)_3$ ,<sup>18</sup>  $VO(C(CH_3)_3)_3$ ,<sup>19</sup>  $VO(O-cyclohexyl)_3$ ,<sup>19</sup>  $VO(OCPh_3)_3$ ,<sup>2c</sup>  $VO(O-1-adamantyl)_3$ ,<sup>2c</sup>  $VO(O-2-adamantyl)_3$ ,<sup>2c</sup>  $VO(O-exo-norbornyl)_3$ ,<sup>2c</sup>  $VO(O-endo-nor-$

bornyl)<sub>3</sub>,<sup>2c</sup>  $VO(O-(R)-bornyl)_3$ ,<sup>2c</sup>  $VO(O-(S)-bornyl)_3$ ,<sup>2c</sup>  $(VO)_4-(CH_3C(CH_2O)_3)_3(OCH_2CH_3)_3$ ,<sup>4c</sup> and  $(VO)_4(CH_3C(CH_2O)_3)_2(OCH_3)_6$ <sup>4c</sup> were prepared for solution- and solid-state characterization using the procedures reported. The connectivity of the latter two compounds are shown in Chart 1. Some of these derivatives have been studied in solution in the past and Table 1 summarizes the <sup>51</sup>V NMR chemical shifts of these derivatives at 50 mM. The less sterically hindered derivatives associate in solution, and the chemical shift accordingly is very sensitive to the concentration of oxovanadium(V) derivative.<sup>2c,4d</sup> Additional details of the characterization have been reported previously<sup>2c,4d,c.16-19</sup> or are included as supplementary material.

**Synthesis and Characterization of the Reaction Product, 1. Formed from *trans*-1,2-Cyclohexanediol and  $VO(OR)_3$ . A Complex with Two Ligands per Vanadium Atom.** Rapid formation of a yellow solid from an orange solution occurs when 1 equiv of  $VO(OCH_2CH_3)_3$  is added to a suspension of 2 equiv of *trans*-1,2-cyclohexanediol (*trans*-CHD) in toluene. The solid product is soluble in  $CH_2Cl_2$  and  $CHCl_3$  and slightly soluble in benzene and toluene. Analysis of an orange solution generated by dissolving the yellow solid product in  $CH_2Cl_2$  gives <sup>51</sup>V NMR resonances at -440, -449, -457, and -461 ppm as well as several minor signals. The variations in signal intensities, as well as the minor signals, suggest several species are present in solution. The chemical shifts, peak ratios, and line widths are indistinguishable from the reaction mixture. This indicates that the product generates an identical mixture of compounds as found in solution before precipitation, and that the yellow solid contains a vanadium to ligand ratio identical to that of the product in the reaction mixture. The complex spectrum suggests that several vanadium species may be generated by means of configurational, conformational, and/or nuclearity changes once the compound is dissolved. <sup>1</sup>H NMR spectra were complex, since several species are in solutions, and the <sup>13</sup>C NMR spectra were not conveniently accessible due to the low solubility of the material. Further characterization of the solution material was therefore omitted.

The solid material was characterized using elemental analysis and IR spectroscopy. The empirical formula,  $VC_{12}H_{23}O_5$ , is consistent with a unit containing two ligands for each oxovanadium

**Table 1.** Solution and Solid-State <sup>51</sup>V NMR Chemical Shift Data for Oxovanadium(V) Alkoxides

ligand	solid	mp, °C	solution <sup>d</sup> $\Delta\delta$ , ppm	solution structure	solid-state $\delta_{iso}$ , <sup>e</sup> ppm	solid structure X-ray
Monoalcohols						
methanol/ <i>n</i> -pentane	yes	100	-594	five <sup>l</sup>	-444.3, -451.7	six
ethanol/ <i>n</i> -pentane	no	5	-604	five	NA	
2-propanol/ <i>n</i> -pentane	no	-6	-634	five	NA	
2-chloroethanol/ <i>n</i> -pentane	yes	NA <sup>a</sup>	-606	five	-505.5	five
<i>tert</i> -butyl alcohol/ <i>n</i> -pentane	yes	NA	-681	four or five	-666.5	
cyclohexanol/hexanes	yes	NA	-627	five		
cyclohexanol/ $CHCl_3$	yes	NA	-616	five		
1-adamantanol/ $CHCl_3$	yes	<i>b</i>	-658	four or five	-703.9	
1-adamantanol/ $CH_3Ph$	yes	<i>b</i>	-661	four or five	-703.9	
2-adamantanol/ $CHCl_3$	yes	<i>c</i>	-605	five	-627.6	
2-adamantanol/ $CH_3Ph$	yes	<i>c</i>	-610	five	-627.6	
<i>exo</i> -norborneol/ $CHCl_3$	yes	63	-612	five	-584.7	
<i>exo</i> -norborneol/hexanes	yes	63	-620	five	-584.7	
<i>endo</i> -norborneol/ $CHCl_3$	yes	58	-594	five	-585.3	
<i>endo</i> -norborneol/hexanes	yes	58	-596	five	-585.3	
triphenylmethanol/ $CH_3Ph$	yes	196	-728	four or five	-700.7	
(1 <i>R</i> )- <i>endo</i> -( $\cdot$ )-borneol/ $CHCl_3$	yes	138	-592	five	-620.1	
(1 <i>R</i> )- <i>endo</i> -( $\cdot$ )-borneol/hexanes	yes	138	-599	five	-620.1	
(1 <i>S</i> )- <i>endo</i> -( $\cdot$ )-borneol/ $CHCl_3$	yes	130	-592	five	-620.1	
(1 <i>S</i> )- <i>endo</i> -( $\cdot$ )-borneol/hexanes	yes	130	-598	five	-620.1	
Diols						
ethylene glycol/ $CH_2Cl_2$	yes	<i>c</i>	-463, -474, -503, -506, -515	five or six	-429.4	
( $\pm$ )-2,3-butanediol/ $CH_2Cl_2$	yes	<i>c</i>	-455, -466, -473	six	-477.8	
2 <i>R</i> ,3 <i>R</i> -butanediol/ $CH_2Cl_2$	yes	<i>c</i>	-482, -487, -490, -499	five or six	-472.7, -484.3	
<i>trans</i> -1,2-cyclohexanediol/ $CH_2Cl_2$	yes	<i>c</i>	-440, -447, -454, -456	six	-438.9	six

<sup>a</sup> NA = not available. <sup>b</sup> Solid sublimates at 156 °C. <sup>c</sup> Solid decomposes. <sup>d</sup> Solutions are 50 mM. <sup>e</sup> Resonance shifts determined by MAS NMR at 298 K.

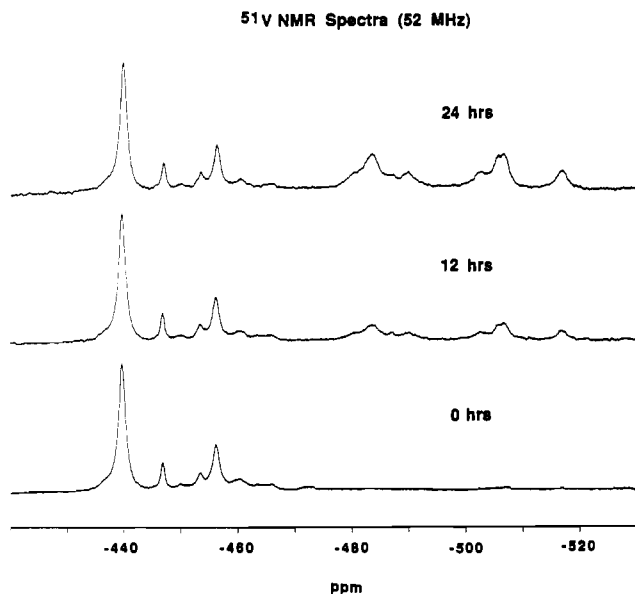


**Figure 1.**  $^{51}\text{V}$  NMR spectra showing decomposition of compound **1** in  $\text{CH}_2\text{Cl}_2$  at  $25^\circ\text{C}$  over a 24-h period.

moiety. The IR spectrum suggests the presence of  $\text{V}=\text{O}$  ( $979\text{ cm}^{-1}$ ) and  $\text{OH}$  ( $3386\text{ cm}^{-1}$ ) moieties; the IR absorbances for this compound are listed in the experimental and other compounds in the supplementary material. No molecular ion was identified by MS due to excessive fragmentation. Solid-state  $^{13}\text{C}$  NMR spectra showed four types of  $\alpha$ -carbons adjacent to either an alkoxide oxygen or a hydroxyl group. Three of these carbons are shifted downfield from the free hydroxyl group of the alcohol, reflecting coordination to the vanadium atom.<sup>22</sup> The four different  $\alpha$ -carbon atoms indicate that the solid-state material contains two types of 1,2-cyclohexanediol units. Only two additional types of carbons were distinguished for the other carbon atoms in the cyclohexane ring.

Further experiments involving various ratios of *trans*-CHD and  $\text{VO}(\text{OCH}_2\text{CH}_3)_3$  were performed. The nature of the product(s) formed from *trans*-CHD depends on the number of equivalents of diol provided to the reaction mixture. A solution in which 1 equiv of diol is added to 1 equiv of  $\text{VO}(\text{OCH}_2\text{CH}_3)_3$  results in an orange solution. No precipitate formed from this solution. The  $^{51}\text{V}$  NMR of the reaction solution shows resonances at  $-484$ ,  $-499$ ,  $-540$ , and  $-601$  ppm. These resonances, which are much further upfield than those found for the 2:1 ligand to metal product, would suggest that the 1:1 product still contains some of the original monodentate alkoxide ligand. The positions of the resonances furthermore varied when different oxovanadium trialkoxide precursors were employed. No differences were observed by  $^{51}\text{V}$  NMR spectroscopy in  $\text{CH}_2\text{Cl}_2$  or toluene when two or more ligands per metal were used.

We examined the changes of a solution mixture of **1** stored under nitrogen atmosphere as a function of time using  $^{51}\text{V}$  NMR spectroscopy. Since these reactions were performed under conditions in which water was rigorously excluded (in a glovebox), hydrolysis reactions should not be observed unless water formed during the reaction. The species that gave rise to the largest resonance at  $-440$  ppm slowly decreased over several days at  $-35^\circ\text{C}$  (Figure 1). While the concentration of the  $-440$  ppm species decreased, signals between  $-480$  and  $-520$  ppm increased in intensity, and the color of the solution turned darker orange-

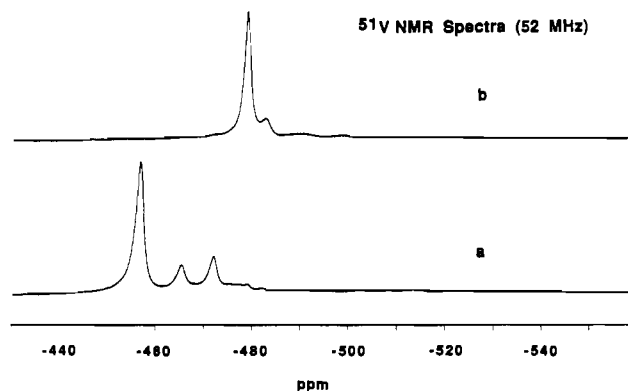


**Figure 2.** (a)  $^{51}\text{V}$  NMR of products formed from the reaction of 1 equiv of  $\text{VO}(\text{OCH}_2\text{CH}_3)_3$  with 2 equiv of  $(\pm)$ -2,3-butanediol. (b)  $^{51}\text{V}$  NMR of products formed from the reaction of 1 equiv of  $\text{VO}(\text{OCH}_2\text{CH}_3)_3$  with 2 equiv of 2*R*,3*R*-butanediol.

brown. These reactions could reflect a change in the oligomerization equilibria and perhaps a reduction of the vanadium(V) center as well. Since higher oxygen coordination around an oxovanadium(V) center often results in a larger downfield shift, the slow appearance and increase of the compounds with resonances upfield may indicate a gradual decrease in average oxygen coordination number around the vanadium atom in the oligomers formed after longer incubation times.

**Reactions of 1.** A solution of **1** at ambient temperature in  $\text{CH}_2\text{Cl}_2$  resulted in reduction of the vanadium(V) center over the course of several days. The oxovanadium(V) alkoxides containing 1,2-diolate ligands are surprisingly unstable, contrary to the bulky oxovanadium(V) trialkoxides<sup>2e</sup> or 1,3-propanediolate derivatives.<sup>4e,11</sup> Perhaps the larger cluster formation with the 1,3-diolates explains the greater stability of these compounds. Compound **1** immediately reacts with water, or other coordinating solvents to generate a large number of products. The solid compound also slowly decomposes at ambient temperature when left exposed to air. The first step of the decomposition turns the solid material orange, presumably due to hydrolysis. The material then turns green, as the vanadium(V) center is reduced, and finally brown. Stored under a nitrogen atmosphere at ambient temperature, the material turns green over a period of several days.

**Synthesis and Characterization of the Reaction Product, 2, from  $\text{VO}(\text{OR})_3$  and  $(\pm)$ -2,3-Butanediol.** Mixing of 2 equiv of  $(\pm)$ -2,3-butanediol (2,3-BD) with 1 equiv of  $\text{VO}(\text{OCH}_2\text{CH}_3)_3$  first formed a clear orange solution, which over 1 h turned yellow while a yellow solid precipitated. A  $^{51}\text{V}$  NMR spectrum of the product in  $\text{CHCl}_3$  reveals major resonances at  $-455$ ,  $-466$ , and  $-473$  ppm (Figure 2a). In addition, weaker resonances are seen between  $-480$  and  $-483$  ppm. No differences were observed by  $^{51}\text{V}$  NMR spectroscopy when comparing the reaction mixture and a solution containing redissolved yellow solid of **2**.

Elemental analysis suggests an empirical of  $\text{VC}_8\text{H}_{17}\text{O}_5$  for the base unit. As seen for compound **1**, the IR spectrum suggests the presence of  $\text{V}=\text{O}$  ( $982$ ,  $989\text{ cm}^{-1}$ ) and  $\text{OH}$  ( $3476\text{ cm}^{-1}$ ) moieties (see Experimental Section and supplementary material for complete list of IR absorption bands in this and related compounds). Two VO signals are observed for this material in contrast to compound **1**. Solid-state  $^{13}\text{C}$  NMR spectra show three different  $\alpha$ -carbons with one signal having twice the intensity of the other two. The coordination induced shift values (CIS) suggest three out of four alkoxide moieties are coordinated to the vanadium atom. Two other  $^{13}\text{C}$  NMR signals for the methyl groups are observed.

**Synthesis and Characterization of the Reaction Product, 3, from  $\text{VO}(\text{OR})_3$  and 2*R*,3*R*-2,3-butanediol.** The reaction of 2 equiv of 2*R*,3*R*-2,3-butanediol (RR-2,3-BD) with 1 equiv of  $\text{VO}(\text{OCH}_2\text{CH}_3)_3$  generated an orange solution from which a yellow, fibrous solid precipitated. A gellike solid formed when the solution was

(21) Kunwar, A. C.; Turner, G. R.; Oldfield, E. *J. Magn. Reson.* **1986**, *69*, 124.

(22) (a) Crans, D. C.; Shin, P. K.; Armstrong, K. A. In *Mechanistic Bioinorganic Chemistry*; Thorp, H. H., Pecoraro, V. L., Eds ACS Symposium Series; American Chemical Society: Washington, DC, in press. (b) Crans, D. C.; Chen, H.; Anderson, O. P.; Miller, M. M. *J. Am. Chem. Soc.* **1993**, *115*, 6769.

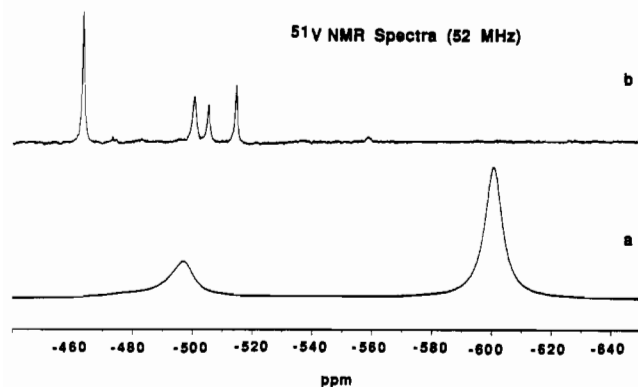


**Figure 3.** (a)  $^{51}\text{V}$  NMR spectrum of reaction between 1 equiv of  $\text{VO}(\text{OCH}_2\text{CH}_3)_3$  with 2 equiv of ethylene glycol; (b)  $^{51}\text{V}$  NMR spectrum of 2:1 ethylene glycol to  $\text{VO}(\text{OCH}_2\text{CH}_3)_3$  Product **4** in  $\text{CH}_2\text{Cl}_2$ .

not agitated. A  $^{51}\text{V}$  NMR spectrum of the product in  $\text{CHCl}_3$  reveals major resonances at  $-482$  and  $-487$  ppm and small broad peaks at  $-490$  and  $-499$  ppm. The signal intensities again suggest the solution contains a mixture of compounds. Although the diol used for the preparation of **3** is simply the enantiomerically pure form of the ligand used for the preparation of **2**, the compound dissolved in  $\text{CH}_2\text{Cl}_2$  has a completely different  $^{51}\text{V}$  NMR spectrum (Figure 2b).

Mass spectroscopic analysis yields a spectrum with the highest mass peak at  $m/e$  537. While the composition of this particular ion is unknown, its presence is indicative of oligomerization in the solid state. In addition, the mass spectrum indicates fragmentation by diolate loss (88 amu) although its complex nature suggests multiple fragmentation pathways. The IR spectrum shows one stretch for  $\text{V}=\text{O}$  at  $989\text{ cm}^{-1}$  and an OH stretch at  $3476\text{ cm}^{-1}$  (see Experimental Section and supplementary material for complete list of IR absorption bands in this and related compounds). The IR spectrum would therefore suggest only one type of  $\text{V}=\text{O}$  and OH moiety. The solid-state  $^{13}\text{C}$  NMR spectrum shows seven different  $\alpha$ -carbon resonances. The signal at 73.6 ppm has twice the intensity of the other six resonances. The CIS values of the six resonances indicate covalent interaction with a vanadium atom. Three additional resonances are observed for the methyl groups.

**Synthesis and Characterization of the Reaction Product, 4, from  $\text{VO}(\text{OR})_3$  and Ethylene Glycol.** Reactions with ethylene glycol are complicated by the low solubility of the diol in noncoordinating solvents; however, we have been successful in obtaining products when ethylene glycol is suspended in toluene. Addition of 1 equiv of  $\text{VO}(\text{OCH}_2\text{CH}_3)_3$  to a suspension of 2 equiv of ethylene glycol yielded a cloudy yellow solution from which a yellow precipitate was isolated. Recording  $^{51}\text{V}$  NMR spectra of the reaction solution as a function of time after addition of the  $\text{VO}(\text{OCH}_2\text{CH}_3)_3$  shows that the transesterification reaction is rapid, and no significant changes in the spectrum are observed after 5 min of reaction time. The  $^{51}\text{V}$  NMR spectrum shows that the mixture contains two major broad signals at  $-496$  and  $-599$  ppm (Figure 3a). The solid is only sparingly soluble in  $\text{CH}_2\text{Cl}_2$  and  $\text{CHCl}_3$ . The precipitate redissolved in  $\text{CH}_2\text{Cl}_2$ , yielding four major  $^{51}\text{V}$  NMR signals at  $-463$ ,  $-503$ ,  $-506$ , and  $-515$  ppm (Figure 3b). An identical  $^{51}\text{V}$  NMR spectrum of the product in  $\text{CH}_2\text{Cl}_2$  was observed when  $\text{VO}(\text{OCH}(\text{CH}_3)_2)_3$  was reacted with ethylene glycol suggesting that the original alkoxide ligands of the oxovanadium(V) trialkoxide are completely replaced.

Characterization of the solid state of this material was conducted using elemental analysis and IR spectroscopy. Elemental analysis indicates an empirical formula of  $\text{VC}_4\text{H}_9\text{O}_5$ . The IR spectrum suggests the presence of  $\text{V}=\text{O}$  ( $950\text{ cm}^{-1}$ ) and OH ( $3435\text{ cm}^{-1}$ ) moieties (see experimental for other IR absorption bands). Solid-state  $^{13}\text{C}$  NMR spectroscopy shows three types of  $\alpha$ -carbon atoms. The peak at 83.7 ppm had double

the intensity of those at 81.8 and 63.7 ppm. One of the carbon atoms has a chemical shift very close to free ethylene glycol. We conclude that three out of four alkoxide moieties are coordinated to the vanadium atom.

Increasing the ethylene glycol concentration to greater than 2 equiv did not change the  $^{51}\text{V}$  NMR spectra or increase the reaction yield. However, the reaction between equimolar amounts of  $\text{VO}(\text{OCH}_2\text{CH}_3)_3$  and ethylene glycol did produce a significantly different  $^{51}\text{V}$  NMR spectrum. The resonances are further upfield and closer to the chemical shift region of the starting oxovanadium(V) trialkoxide. In addition, these chemical shifts changed when other  $\text{VO}(\text{OR})_3$  compounds (such as  $\text{VO}(\text{OCH}_3)_3$  and  $\text{VO}(\text{OCH}(\text{CH}_3)_2)_3$ ) were used as starting materials.

The rate in which the product is formed is dependent on the type of terminal alkoxide ligand that is being replaced. The sterically bulky 2-propanolato ligand is replaced by diol much slower than ethanolato or methanolato ligands. In  $^{51}\text{V}$  NMR studies, methanolato replacement is fast enough that the resonance for  $\text{VO}(\text{OCH}_3)_3$  has completely disappeared within the time it takes to prepare the sample and record the  $^{51}\text{V}$  NMR spectrum. Although none of these systems have been studied kinetically, the greater stability and lower reactivity of oxovanadium(V) trialkoxides of sterically hindered alcohols has been described previously.<sup>2c</sup>

**Infrared Spectral Analysis of Compounds 1–4.** IR spectra of compounds **1–4** show very broad and intense absorption bands from  $3476$  to  $3386\text{ cm}^{-1}$ . These bands, attributed to hydroxyl stretching vibrations, are shifted to lower frequencies than normally found for free hydroxyl groups. This is presumably a result of weak interaction with a vanadium atom. Absorption bands attributable to the  $\text{V}=\text{O}$  moiety are found from  $989$  to  $950\text{ cm}^{-1}$ . These signals are within the region found for many oxovanadium(V) alkoxides and polyoxovanadates compounds. The presence of the  $\text{V}=\text{O}$  bands eliminates the possibility for structures without such functionalities. In the past, increasing alkyl substitution correlated with a decrease in the observed  $\text{V}=\text{O}$  stretching frequency.<sup>23</sup> Indeed, such a trend is found for compounds **1–3**. Compound **4**, which has the least amount of alkyl substitution, does not conform to this trend since it has a  $\text{V}=\text{O}$  stretching frequency considerably lower than the others. In fact, the  $\text{V}=\text{O}$  stretching frequency of **4** is shifted far enough away from those of compounds **1–3**, as well as other reported  $\text{V}=\text{O}$  stretches in  $\text{VO}(\text{OR})_3$  and polyoxovanadate compounds, that its structure may differ from the other three.

In summary, any geometry that does not contain a  $\text{V}=\text{O}$  moiety is not consistent with the observed IR data. Furthermore, the IR spectra do not support the presence of free hydroxyl groups in compounds **1–4** since none of these compounds have the distinct sharp bands characteristic for free hydroxyl groups.

**Solid-State  $^{51}\text{V}$  NMR Characterization: Data Analysis.** The  $^{51}\text{V}$  nucleus ( $I = 7/2$ ) has a nuclear electric quadrupole moment of moderate size which influences the NMR spectra in the solid state and must be taken into account in the spectrum analysis. The interaction of this quadrupole moment with electric field gradients created by the chemical bonding environment lifts the degeneracy of the seven allowed Zeeman transitions. To first-order perturbation analysis the resonance splits into a central transition ( $m = +1/2 \rightarrow m = -1/2$ ) that remains unaffected by the quadrupole interaction, and six broad "satellite" powder patterns that are shifted and greatly broadened by the anisotropy of the quadrupolar perturbation. In the case of  $^{51}\text{V}$  solid-state NMR, the central transition generally displays characteristic powder patterns reflecting the anisotropy of the chemical shift interaction and dipole-dipole couplings, the latter modifying the spectra in a minor way. Magic-angle spinning (MAS) succeeds

(23) Voronkov, M. G.; Shergina, N. I.; Lapsin, A. F. *Bull. Acad. Sci. USSR, Div. Chem. Sci. (Engl. Transl.)* **1973**, *12*, 2745.

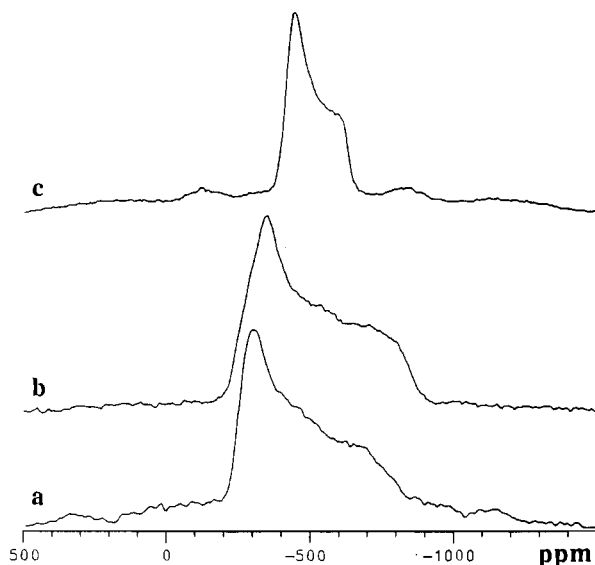


**Figure 4.** 79.0-MHz  $^{51}\text{V}$  wide-line NMR spectra of crystallographically characterized oxovanadium(V) alkoxides: (a)  $\text{VO}(\text{OCH}_3)_3$ ; (b)  $(\text{VO})_4(\text{CH}_3\text{C}(\text{CH}_2\text{O})_3)_2(\text{OCH}_3)_6$ ; (c)  $\text{VO}(\text{OCH}_2\text{CH}_2\text{Cl})_3$ .

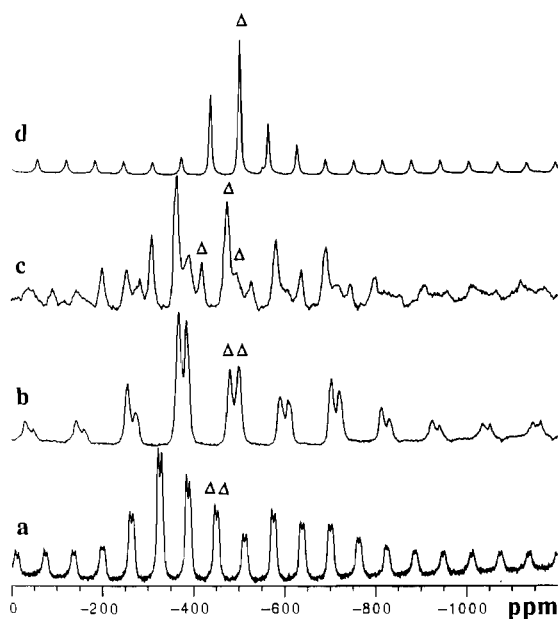


**Figure 5.** 79.0-MHz  $^{51}\text{V}$  MAS-NMR spectra of crystallographically characterized oxovanadium(V) alkoxides: (a)  $\text{VO}(\text{OCH}_3)_3$ ; (b)  $(\text{VO})_4(\text{CH}_3\text{C}(\text{CH}_2\text{O})_3)_2(\text{OCH}_3)_6$ ; (c)  $(\text{VO})_4(\text{CH}_3\text{C}(\text{CH}_2\text{O})_3)_3(\text{OCH}_2\text{CH}_3)_3$ ; (d)  $\text{VO}(\text{OCH}_2\text{CH}_2\text{Cl})_3$ . The MAS center bands are denoted by the symbol  $\Delta$ .

in narrowing these powder patterns effectively, resulting in a central band at the isotropic chemical shift position and spinning sidebands appearing at integer multiples of the spinning frequency. MAS also narrows effectively the first-order quadrupolar satellite powder patterns, resulting in wide spinning sideband manifolds.

In second-order perturbation analysis, the resonance frequency of the central  $+1/2 \rightarrow -1/2$  transition is rendered orientationally dependent due to the anisotropy of the quadrupolar interaction. The resulting line shapes are quite complicated, depending on the principal values of the chemical shift and quadrupolar tensors and their mutual orientation. In such cases, MAS is less effective for line-narrowing. Characteristic line shapes for the MAS centerbands are observed, from which the quadrupolar Hamiltonian can be evaluated.

Figures 4–9 summarize typical wide-line and MAS-NMR spectra obtained for the compounds investigated in the present study. The static spectra are dominated by the central  $+1/2 \rightarrow$

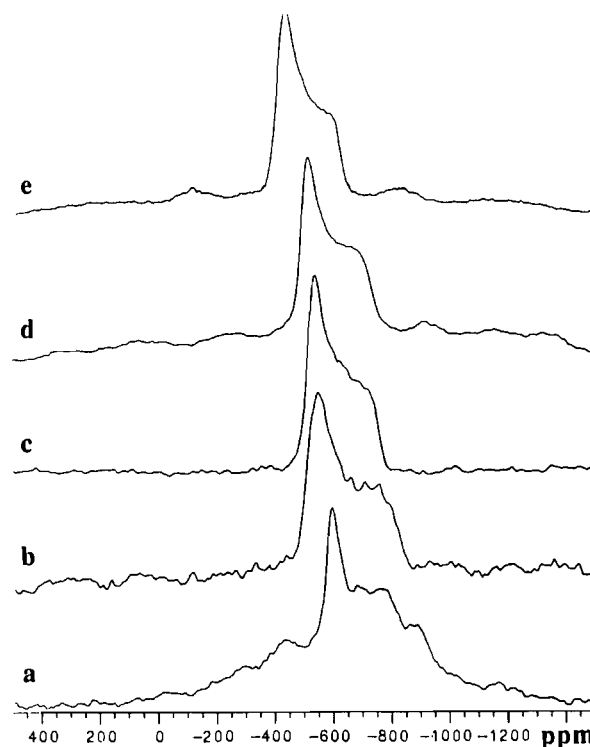


**Figure 6.** 79.0-MHz  $^{51}\text{V}$  wide-line NMR spectra of various known oxovanadium(V) alkoxides, previously characterized: (a)  $\text{VO}(\text{O}-1\text{-adamantyl})_3$ ; (b)  $\text{VO}(\text{O}-2\text{-adamantyl})_3$ ; (c)  $\text{VO}(\text{O}-\text{cyclohexyl})_3$ ; (d)  $\text{VO}(\text{O}-\text{endo-norbornyl})_3$ ; (e)  $\text{VO}(\text{OCH}_2\text{CH}_2\text{Cl})_3$ .

$-1/2$  transitions, with weaker features due to the other Zeeman transitions affected by quadrupolar broadening. At both 79.0 and 131.5 MHz, the central transitions have the typical line shapes of anisotropic chemical shift powder patterns and bear little evidence of second-order quadrupole effects. Indeed, excellent fits to the static spectra can be obtained in most cases, by assuming that the line shapes are completely dominated by the chemical shift anisotropy. Table 2 lists approximate chemical shift tensor components, which were extracted from the static spectra by comparison with computer simulations using the FTNMR software package. The chemical shift tensor values estimated in this fashion are reported using the convention  $\delta_{11} > \delta_{22} > \delta_{33}$ . In principle it might be possible to obtain more accurate data by resorting to complex line-shape simulation routines, incorporating noncoincident quadrupole and chemical shift tensors.<sup>24</sup> However, such a procedure raises the number of adjustable parameters from three to eight and appears not to be justified in view of the fairly good agreement already obtained when neglecting second-order quadrupolar effects on the static line shape.

The MAS-NMR spectra show generally sharp and well-resolved peaks associated with the central  $+1/2 \rightarrow -1/2$  transitions. Because the spinning frequencies employed are generally smaller than the magnitude of the chemical shift anisotropy, intense spinning sideband patterns are produced in addition to the central resonance. For all compounds with multiple vanadium sites, the chemical shift tensor components were obtained from an intensity analysis of these spinning sideband patterns, using the procedure of Herzfeld and Berger.<sup>25</sup> In addition, wide sideband patterns of lower intensity appear in these spectra due to the MAS-modulation of first-order quadrupolar powder patterns. Although the sharp and well-resolved MAS center bands indicate that in most cases second-order quadrupolar effects are rather weak, those effects are detectable by a field-dependent contribution as shown in eq 1.

(24) Power, W. P.; Wasylshen, R. E.; Mooibroik, S.; Pettit, B. A.; Danchura, W. *J. Phys. Chem.* **1990**, *94*, 591.

(25) Herzfeld, J.; Berger, A. E. *J. Chem. Phys.* **1980**, *73*, 6021.



$$\delta_{\text{exp}} = \delta_{\text{iso}} + \delta^{(2)} \quad (1)$$

For a spin-7/2 nucleus, the second order quadrupolar shift  $\delta^{(2)}$  is given by eq 2, where  $\nu_0$  is the nuclear Larmor frequency and

$$\delta^{(2)} \text{ [ppm]} = -2551 \nu_0^{-2} (e^2qQ/h)^2 \cdot (1 + \eta^2/3) \quad (2)$$

$e^2qQ/h$  and  $\eta$  are the principal component and the asymmetry parameter, respectively, of the nuclear electric quadrupolar interaction. Thus, field-dependent measurements of  $\delta_{\text{exp}}$  afford the isotropic chemical shifts as well as the product  $(e^2qQ/h)^2(1 + \eta^2/3)^{1/2}$  characterizing the strength of the nuclear electric quadrupolar interaction. This analysis is summarized in Table 2.

**Solid-State  $^{51}\text{V}$  NMR Characterization: I. Simple Oxovanadium(V) Alkoxides.** Figures 4–7 shows representative  $^{51}\text{V}$  MAS and wide-line NMR spectra of simple oxovanadium(V) alkoxides. If more than one product were present in the materials, more complex spectra would have resulted than those shown in Figures 4–7. The solid-state molecular geometries of several of these compounds (Figures 4 and 5) are known from single-crystal X-ray diffraction,<sup>4b,d,6</sup> while the geometries of others (Figures 6 and 7) have been inferred from the NMR solution state data.<sup>2e,4d,16–19</sup> In the compound  $\text{VO}(\text{OCH}_3)_3$  the vanadium atoms are octahedrally coordinated in a dimeric unit with two non-bridging and three doubly bridging methoxide ligands. Each dimeric unit is coordinated to other units connecting the structure in a polymeric pattern. The structure was solved and reported despite the disordered crystals resulting in an  $R$  value of 0.168.<sup>6</sup> The solid state MAS-NMR spectrum (Figure 4a) shows two closely spaced resonances in a ratio of 1:1. This result is in accord with the crystallographic study indicating that within each dinuclear unit, the vanadium atoms are structurally inequivalent.

Parts b and c of Figure 5 show MAS-NMR results for  $(\text{VO})_4(\text{CH}_3\text{C}(\text{CH}_2\text{O})_3)_2(\text{OCH}_3)_6$  and  $(\text{VO})_4(\text{CH}_3\text{C}(\text{CH}_2\text{O})_3)_3(\text{OCH}_2\text{CH}_3)_3$ . The structure of  $(\text{VO})_4(\text{CH}_3\text{C}(\text{CH}_2\text{O})_3)_2(\text{OCH}_3)_6$  has been refined to an  $R$  value of 0.046 and consists of tetramers with two crystallographically inequivalent six-coordinated vanadium sites.<sup>4e</sup> In agreement with this structure, the solid-state  $^{51}\text{V}$  NMR spectra show two distinct peak patterns in a 1:1 ratio. The crystal structure of  $(\text{VO})_4(\text{CH}_3\text{C}(\text{CH}_2\text{O})_3)_3(\text{OCH}_2\text{CH}_3)_3$  as refined to an  $R$  value of 0.076, consists of tetramers with four inequivalent six-coordinated vanadium sites.<sup>4e</sup> Consistent with this information, the solid-state  $^{51}\text{V}$  NMR spectra reveal three distinct peak patterns in a 2:1:1 ratio (two of the vanadium sites are not resolved from each other).

In the three model compounds described above, the structural similarities of the respective vanadium(V) centers are reflected in common chemical shift parameters: the distorted six-coordinated ligand environments of the vanadium center are characterized by near-axially symmetric  $^{51}\text{V}$  chemical shift tensors with  $\delta_{\parallel}$  in the range  $-800$  to  $-900$  ppm and  $\delta_{\perp}$  larger than  $-300$  ppm. These parameters also agree rather well with those obtained for other six-coordinated vanadium compounds.<sup>13</sup> The near-axial chemical shift tensor property in these three model compounds is somewhat unexpected, because their crystal structures do not reveal the presence of a higher symmetry axis at the vanadium center. However, the significantly shorter length of the  $\text{V}=\text{O}$  bond compared to any of the other vanadium–oxygen bond lengths suggests that the shielding along the  $\text{V}=\text{O}$  bond is significantly different compared to that perpendicular to it. Thus, we anticipate that  $\delta_{33}$  approximates the chemical shift along the  $\text{V}=\text{O}$  double bond in all of these compounds.

The crystal structure of  $\text{VO}(\text{OCH}_2\text{CH}_2\text{Cl})_3$  has been recently reported by Rehder.<sup>4d</sup> The vanadium is pentacoordinate due to a fifth bridging alkoxide ligand ( $\text{V}-\text{OR} = 2.261(2)$  Å), resulting in a dinuclear molecule. The MAS-NMR and static spectra reveal a near-axially symmetric chemical shift tensor, with a

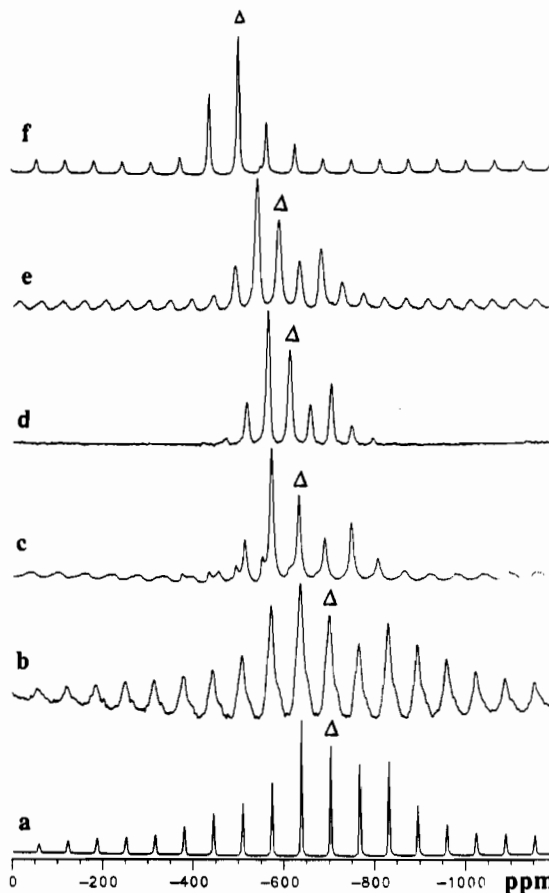


**Figure 7.** 79.0-MHz  $^{51}\text{V}$  MAS-NMR spectra of various known oxovanadium(V) alkoxides: (a)  $\text{VO}(\text{O}-1\text{-adamantyl})_3$ ; (b)  $\text{VO}(\text{OCPH}_3)_3$ ; (c)  $\text{VO}(\text{O}-2\text{-adamantyl})_3$ ; (d)  $\text{VO}(\text{O}-\text{cyclohexyl})_3$ ; (e)  $\text{VO}(\text{endo-norbornyl})_3$ ; (f)  $\text{VO}(\text{OCH}_2\text{CH}_2\text{Cl})_3$ . The MAS center bands are denoted by the symbol  $\Delta$ .

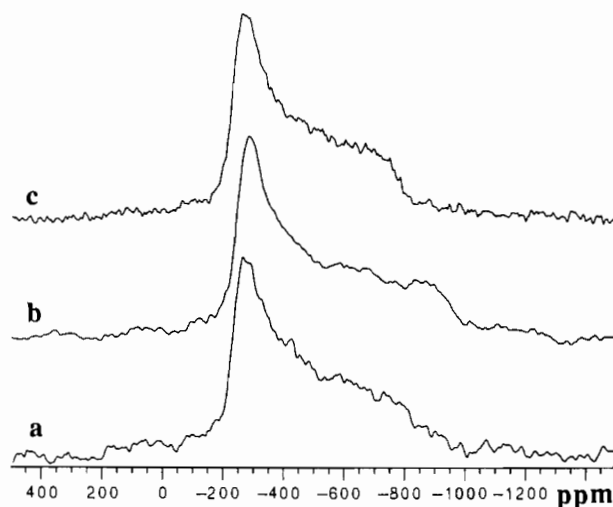


**Figure 8.** 79.0-MHz wide-line NMR spectra of compounds 1 (a), 2 (b), and 4 (c).

substantially smaller anisotropy compared to the compounds above (see Figure 4c). The preparation and characterization of other oxovanadium(V) alkoxides with less than six ligands around the vanadium has been previously reported.<sup>2e,4b,16–19</sup> Although no X-ray crystal structures of oxovanadium(V) alkoxides with tetrahedral vanadium are available, they have been studied extensively in solution.<sup>2e,16–19</sup> Representative solid-state NMR spectra are shown in Figure 6. The compounds with alkoxide moieties from 2-adamantanol, (*R*)- and (*S*)-borneol, *exo*- and *endo*-norborneol, cyclohexanol, and *tert*-butyl alcohol all show

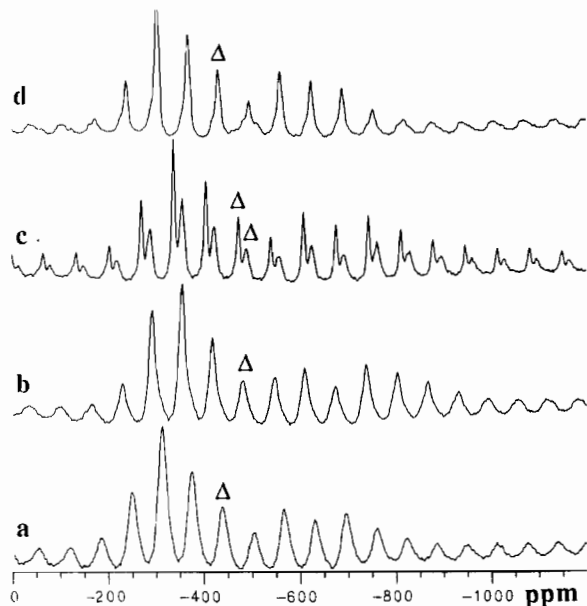


**Figure 9.** 79.0-MHz  $^{51}\text{V}$  MAS-NMR spectra of compounds **1** (a), **2** (b), **3** (c), and **4** (d). The MAS centerbands are denoted by the symbol  $\Delta$ . chemical shift anisotropies comparable to that found in  $\text{VO}(\text{OCH}_2\text{CH}_2\text{Cl})_3$ . There is considerable variation, however, in the isotropic chemical shift, from  $-500.5$  ppm in  $\text{VO}(\text{OCH}_2\text{CH}_2\text{Cl})_3$  to  $-669.3$  ppm in  $\text{VO}(\text{OC}(\text{CH}_3)_3)_3$ . We interpret this behavior to indicate that the general vanadium–oxygen coordination geometries in this group of compounds are basically all similar except for the strength of intermolecular interactions resulting in the fifth V–O bond. Consistent with the chemical shift trends reported previously,<sup>26</sup> we suggest that the strength of the fifth V–O bond arising from intermolecular interactions diminishes as the isotropic  $^{51}\text{V}$  chemical shift moves upfield. Thus, the compounds within this group are probably monomeric in the solid state, with intermolecular V–O interactions that are perceptible but substantially weaker than in  $\text{VO}(\text{OCH}_2\text{CH}_2\text{Cl})_3$ .

The oxovanadium(V) alkoxides from 1-adamantanol and triphenylmethanol are characterized by the largest upfield chemical shifts ( $< -700$  ppm) within this series. In addition, these materials are distinguished by negligible second-order quadrupolar shifts indicating that the nuclear electric quadrupole coupling is rather weak. The MAS peak patterns, associated with the central transitions and the quadrupolar satellites are not clearly resolvable from each other, and no accurate chemical shift tensor information is obtainable for these molecules. On the basis of this distinct spectroscopic behavior, we conclude that these two compounds are essentially monomeric in character in the solid state, with negligible secondary V–O interactions. This behavior is not unexpected, since these materials are monomeric in solution,<sup>26</sup> presumably because the approach of a fifth oxygen ligand into the binding sphere of the vanadium center is sterically most difficult.

**Solid-State  $^{51}\text{V}$  NMR Characterization: Oxo–Vanadium(V) Alkoxides from 1,2-Diols.** The solid-state  $^{51}\text{V}$  NMR data base established above for the simple oxovanadium(V) alkoxides now allows for a discussion of the local vanadium coordination environments in the new 1,2-diolato complexes **1–4**. Figures 8 and 9 summarize the data, obtained under both static and MAS conditions. The isotropic and anisotropic chemical shift parameters extracted from the static and the MAS-NMR spectra reveal common spectroscopic behavior for compounds **1–4**. Comparison with the data base discussed above indicates that the vanadium atoms are six-coordinated in all four complexes.

The 79.0 MHz MAS-NMR spectra discern only single vanadium sites in compounds **1**, **2**, and **4**. However, substantial

line broadening effects signify considerable disorder in the crystal structure of compound **1**. In contrast, compound **3**, prepared from enantiomerically pure 2*R*,3*R*-butanediol, reveals two MAS peak patterns in an approximate area ratio of 1:1 as verified by peak integration. Additional details of the MAS center bands are apparent in the better-resolved 131.5 MHz spectra of both compounds **2** and **3** (Figure 10). Compound **2** shows more line broadening, and the main peak at  $-480$  ppm is accompanied by two distinct shoulders that are located in the vicinity of the two peaks observed in compound **3**. Compound **2** also shows a minor feature at  $-497$  ppm. The ratios of major peak to shoulders were identical in several sample preparations, and storage under nitrogen (without decomposition) did not affect the signal distribution. The shoulders observed for compound **3** are therefore not a result of isomerization in the solid state. These observations are consistent with the following interpretation: the vanadium complex containing enantiomerically pure 2*R*,3*R*-butanediolato ligands is an oligomer with two crystallographically distinct vanadium sites. The situation is different in compound **2**. The two diol residues per vanadium atom give rise to formation of enantiomeric and diastereomeric monomeric units:  $\text{O}=\text{V}(\text{R},\text{R}-2,3\text{-BD})_2$ ,  $\text{O}=\text{V}(\text{S},\text{S}-2,3\text{-BD})_2$ , and  $\text{O}=\text{V}(\text{R},\text{R}-2,3\text{-BD})(\text{S},\text{S}-2,3\text{-BD})$ . If these monomeric units dictated the spectra, the feature at  $-497$  ppm would be absent and less line broadening would be expected. The features presumably arise from interactions among the various units upon oligomerization in the solid state.

Despite the information obtained by solid-state  $^{51}\text{V}$  NMR spectroscopy, additional information would be desirable, and solid-state  $^{13}\text{C}$  NMR spectroscopy was carried out to further characterize the new materials.

**Solid-State  $^{13}\text{C}$  NMR Characterization.**  $^{13}\text{C}$  CPMAS NMR spectra of  $\text{VO}(\text{OCH}_3)_3$ ,  $\text{VO}(\text{OC}(\text{CH}_3)_3)_3$ , and the oxovanadium(V) 1,2-diolato derivatives were recorded and are shown in Figure 11. The chemical shift data for the latter compounds are given in the Experimental Section, and the quantitative ratios of the signals are described in the Results. Due to the various relaxation processes involved in the generation of the signal, in general, signal intensities in CPMAS NMR spectra cannot be viewed as quantitative. For the present samples, however, systematic investigations as a function of contact time did not show strong differences in relative intensities among various sites and types of protonated carbon atoms. Thus, the relative peak intensities presumably approximate relative site populations.

A common feature to most of the spectra shown in Figure 11 are the shifts of the resonances assigned to the ligand carbon atoms in the  $\alpha$ -position. This feature is illustrated in Figure 12 where the CIS value  $\Delta\delta$  ( $\Delta\delta = \delta_{\alpha\text{-carbon in complex}} - \delta_{\alpha\text{-carbon in free ligand}}$ ) is plotted for each  $\alpha$ -carbon signal of the compounds examined. CIS values have been used for solution studies of vanadium(V) complexes;<sup>22</sup> however, Figure 12 shows this type of analysis is also very informative in the solid state. The oxygen atom in the alkoxide groups can be noncoordinated, coordinated to one vanadium atom, or bridged between two (or even three) vanadium atoms. The downfield shifts of the  $\alpha$ -carbons fall into distinct groups. The weakly interacting hydroxide moiety has an  $\alpha$ -carbon with a  $\Delta\delta$  value close to zero. The oxygen atom coordinated to one vanadium atom has a  $\Delta\delta$  value for the  $\alpha$ -carbon around 15–20 ppm, and the oxygen atom bridging between two vanadium atoms has  $\Delta\delta$  value for the  $\alpha$ -carbon around 20–30 ppm. Specifically, the furthest downfield resonances in  $\text{VO}(\text{OCH}_3)_3$  at 77.6 and 76.3 ppm are assigned to the carbon atoms adjacent to an oxygen that is bridging two vanadium atoms. The resonances at 72.0 and 70.0 ppm are assigned to the carbon atoms adjacent to oxygen atoms that form a weaker bridge between the dimeric units. The last two resonances at 66.9 and 66.2 ppm are assigned to the methyl groups bonded to the nonbridging oxygen atoms (Figure 12). In contrast, the  $^{13}\text{C}$  CPMAS NMR spectrum of the monomeric  $\text{VO}(\text{OC}(\text{CH}_3)_3)_3$  is very simple. The absence of

(26) Lachowicz, A.; Thiele, K.-H. *Z. Anorg. Allg. Chem.* **1977**, *434*, 271.



**Table 2.** Solid-State  $^{51}\text{V}$  NMR Data for Oxovanadium(V) Alkoxides<sup>a-c</sup>

ligand	$\delta(79.0)$ , ppm ( $\pm 0.5$ )	$\delta(131.5)$ , ppm ( $\pm 0.5$ )	$\delta_{\text{iso}}$ , ppm ( $\pm 1.0$ )	$e^2qQ/h(1 + \eta^2/3)^{1/2}$ , MHz ( $\pm 0.3$ )	$\delta_{11}$ , ppm ( $\pm 20$ )	$\delta_{22}$ , ppm ( $\pm 20$ )	$\delta_{33}$ , ppm ( $\pm 20$ )	vanadium coord no.
$\text{CH}_3\text{OH}$	-448.5	-445.8	-444.3 (1)	3.3	-250	-305	-780	six (X-ray)
$\text{CH}_3\text{C}(\text{CH}_2\text{OH})_3$ , and $\text{CH}_3\text{OH}$	-454.8	-452.8	-451.7 (1)	3.1	-250	-305	-780	six (X-ray)
	-481.9	-478.8	-477.0 (1)	3.5	-210	-340	-890	six (X-ray)
	-501.2	-498.9	-497.6 (1)	3.0	-290	-340	-870	six (X-ray)
$\text{CH}_3\text{C}(\text{CH}_2\text{OH})_3$ , and $\text{CH}_3\text{CH}_2\text{OH}$	-420.6	-415.5	-412.5 (1)	4.4	-50	-270	-930	six (X-ray)
	-476.9	-470.1	-466.2 (2)	5.1	-130	-400	-880	six (X-ray)
	-497.1	-490.9	-487.4 (1)	4.9	-150	-360	-960	six (X-ray)
<i>trans</i> -1,2-cyclohexanediol	-440.0	-439.3	-438.9	1.6	-225	-275	-850	(six)
( $\pm$ )-2,3-butanediol	-484.0	-480.2	-477.8	4.0	-250	-300	-950	(six)
2 <i>R</i> ,3 <i>R</i> -butanediol	-475.4	-473.7	-472.7 (1)	2.6	-170	-370	-880	(six)
	-491.5	-486.9	-484.3 (1)	4.2	-180	-350	-930	(six)
ethylene glycol	-433.3	-430.8	-429.4	3.1	-240	-290	-800	(six)
$\text{ClCH}_2\text{CH}_2\text{OH}$	-502.2	-501.1	-500.5	2.1	-420	-450	-640	five (X-ray)
<i>tert</i> -butyl alcohol	-669.3	-667.5	-666.5	2.6	-555	-575	-875	(four or five)
cyclohexanol	-614.2	ND <sup>b</sup>	ND	ND	-515	-540	-770	(four or five)
1-adamantanol	-704.2	-704.0	-703.9	0.9	<i>a</i>	<i>a</i>	<i>a</i>	(four or five)
2-adamantanol	-634.2	-630.0	-627.6	4.0	-500	-550	-825	(four or five)
<i>exo</i> -norborneol	-588.1	-585.9	-584.7	2.9	-490	-520	-750	(four or five)
<i>endo</i> -norborneol	-588.0	-586.3	-585.3	2.6	-495	-522	-740	(four or five)
borneol	-622.9	-621.1	-620.1	2.6	-525	-550	-825	(four or five)
triphenylmethanol	-704.2	-700.9	-700.7	0	<i>a</i>	<i>a</i>	<i>a</i>	(four or five)

<sup>a</sup> Chemical shift anisotropy too small to be determined. <sup>b</sup> ND: not determined. <sup>c</sup> Numbers in parentheses denote relative site populations for compounds with multiple peaks.

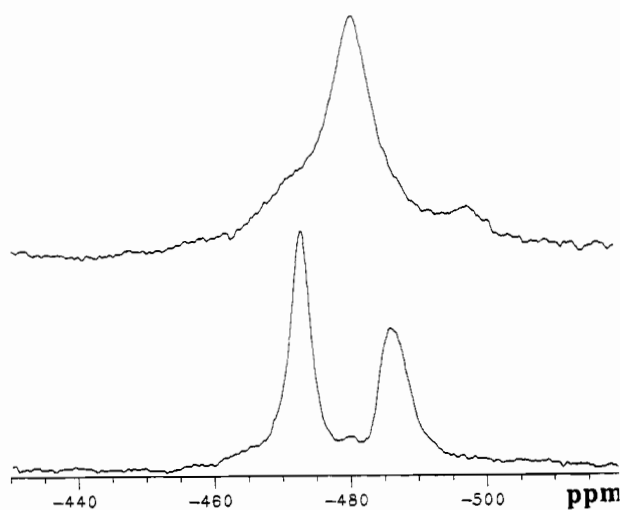


**Figure 10.** 131.5-MHz  $^{51}\text{V}$  MAS-NMR center bands of compounds **2** (top) and **3** (bottom).

alkoxide site inequivalencies suggest the absence of bridging alkoxides and indicates that the single resonance observed near 90 ppm can be assigned to the  $\alpha$ -carbon atom adjacent to the coordinating, nonbridging oxygen atom. In addition, the spectra show that one of the three methyl resonances is strongly downfield-shifted, presumably due to a magnetic anisotropy effect arising from interactions with a neighboring  $\text{V}=\text{O}$  group.

The  $^{13}\text{C}$  CPMAS NMR spectra recorded of  $\text{VO}(\text{OCH}_3)_3$  and  $\text{VO}(\text{OC}(\text{CH}_3)_3)_3$  illustrated the ability of this method to accurately describe the connectivity in the solid state material. Interpretation of the solid-state  $^{13}\text{C}$  NMR spectra thus should assist in further describing the geometries of compounds **1–4**. First, the number of unique  $\alpha$ -carbon atoms and their association with the vanadium is determined. Figure 12 illustrates the weak interaction (if any) of one hydroxyl group per two diol units. Furthermore, the double bridging mode of one  $\alpha$ -carbon per two diol units in compound **1–3** is clear, whereas ethylene glycol contains one doubly bridging  $\alpha$ -carbon per diol. This interpretation is substantiated by plotting the  $\Delta\delta$  for  $\text{VO}(\text{OCH}_3)_3$  (entry a). Entry b shows the shift observed for  $\text{VO}(\text{OC}(\text{CH}_3)_3)_3$  which is presumed to contain a tetrahedral vanadium atom.

The solid-state  $^{13}\text{C}$  NMR spectra of all the oxovanadium(V) diolate complexes have features that are similar to  $\text{VO}(\text{OCH}_3)_3$

suggesting similar structural arrangements and coordination modes for most of the oxygen atoms to which the  $\alpha$ -carbons are bound. However, there is one important difference: for each of the diolate complexes, one resonance assigned to an  $\alpha$ -carbon, accounting for roughly one-fourth of the overall alkoxide signal intensity, is shifted significantly upfield with respect to the other  $\alpha$ -carbon resonances. The  $^{13}\text{C}$  chemical shift of these resonances is very close to that observed for the free ligand. Accordingly this  $\alpha$ -carbon is assigned to an  $\alpha$ -carbon bound to a free or weakly interacting hydroxyl group. The number of observable  $^{13}\text{C}$  peaks for  $\alpha$ -carbons in each compound are a reflection of the ligand arrangement in the solid state and can be used to help determine the structure of the compound. The detailed analysis will be discussed below.

Solution CIS values for the  $\alpha$ -carbons of selected compounds including  $\text{VO}(\text{OCH}_3)_3$ ,  $\text{VO}(\text{O-}i\text{exo-norbornyl})_3$ , and  $\text{VO}(\text{OC}(\text{CH}_3)_3)_3$  have been included in Figure 12 (entries c–e). A comparison of the CIS value for  $\text{VO}(\text{OCH}_3)_3$  in solution with those observed in the solid (entries c and a) shows that the solution CIS value represents an average of those observed in the solid state. In the case of  $\text{VO}(\text{OC}(\text{CH}_3)_3)_3$ , however, a larger CIS value is observed in the solid state than in the solution.

## Discussion

The  $^{51}\text{V}$  solution NMR spectra of compounds **1–4** contain several signals and complicate studies of the species in solution. The large number of species found in solution of compounds **1–4** is presumably a result of alkoxide exchange processes and of several structures of similar energy. Factors such as steric bulk of an alkoxide ligand and the number of alkoxy oxygens per ligand in an oxovanadium(V) molecule effect motional processes. Nonbulky terminal alkoxide ligands such as ethoxide in  $\text{VO}(\text{OCH}_2\text{CH}_3)_3$  rapidly exchange whereas exchange between adamantoxide ligands in  $\text{VO}(\text{O-1-adamantyl})_3$  molecules is slow.<sup>2e,12,26</sup> Alkoxide compounds with bidentate ligands have increased structural and functional exchange possibilities. Characterization of compounds **1–4** in the solid state will assist in defining these complex systems. Since these materials resist characterization by X-ray crystallography, other methods such as solid-state  $^{51}\text{V}$  NMR must be used.

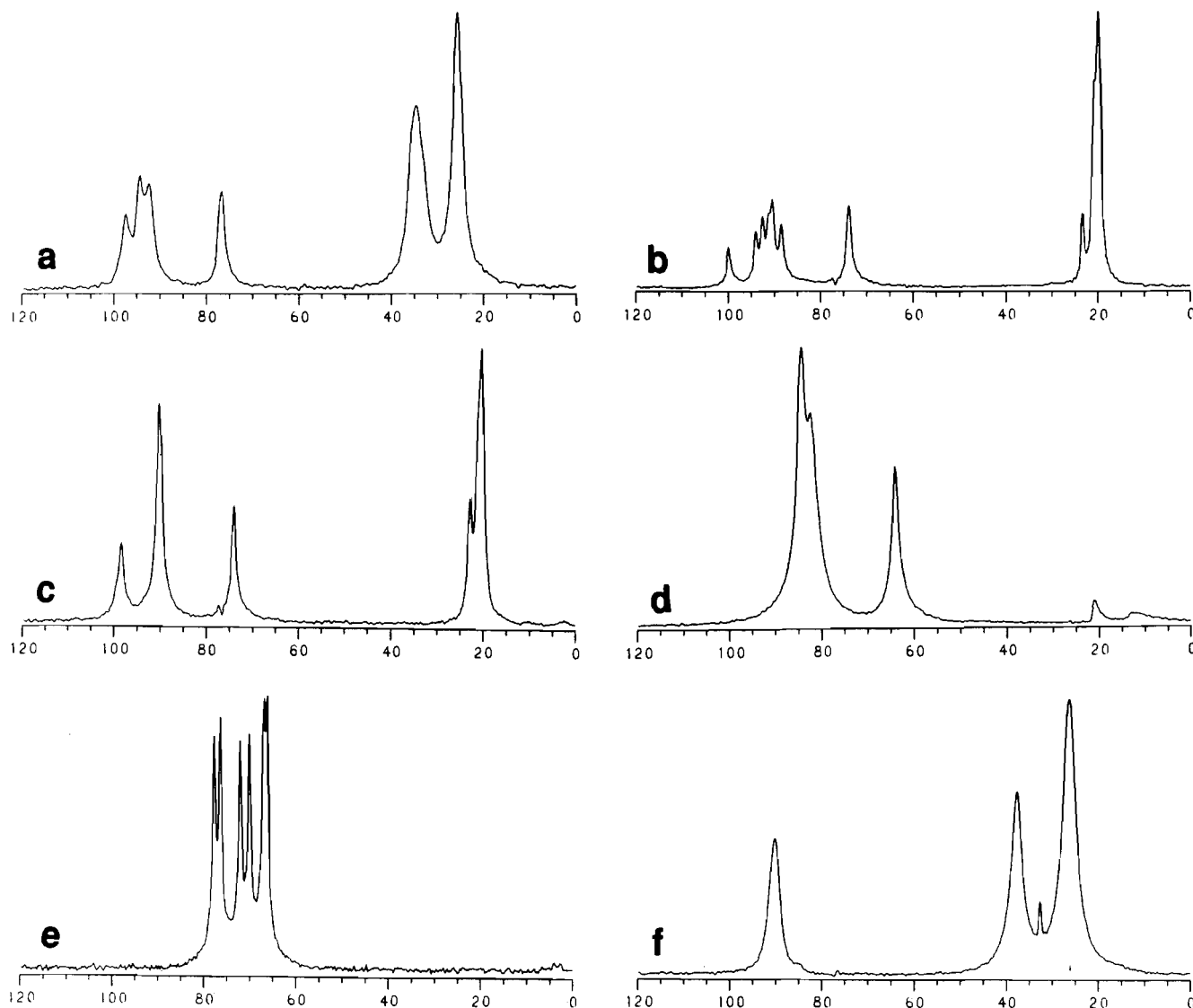
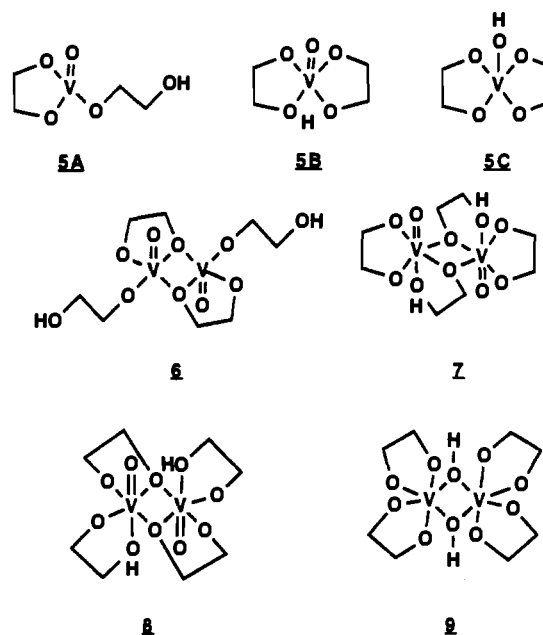


**Figure 11.** 75-MHz  $^{13}\text{C}$  CPMAS NMR spectra of oxovanadium(V) diol complexes: (a) **1**; (b) **3**; (c) **2**; (d) **4**; (e)  $\text{VO}(\text{OCH}_3)_3$ ; (f)  $\text{VO}(\text{OC}(\text{CH}_3)_3)_3$ .

The solid-state  $^{51}\text{V}$  NMR spectra suggest that compounds **1–4** contain vanadium in a six-coordinate environment. Compounds **1** and **4** contain structures in which only one unique type of vanadium atom is present. Elemental analysis reveals that the empirical formula of each of the compounds contains the same number of carbon atoms that would be acquired for two diol ligands per vanadium atom. Although no direct analysis for oxygen was performed, once contributions for C, H, and V were accounted for, the remaining fraction correlated with five oxygen atoms per vanadium. Since the syntheses were conducted in toluene, no additional atoms would be expected to be present in the materials isolated. Compounds **1–4** must therefore all be described by a base unit consisting of VO, two diolates, and one proton. Examples of possible structures for the base units are **5A**, **5B**, and **5C**. The mass spectroscopic data discussed above, as well as the solid state  $^{51}\text{V}$  NMR data, do not rule out, the formation of oligomeric or polymeric structures. Specifically, a trimeric unit was observed in the mass spectrum of compound **3**. Structural precedence for oxovanadium(V) alkoxides include dinuclear,<sup>4a–4d</sup> tetranuclear,<sup>4e,5</sup> hexameric<sup>3</sup> and polymeric structures<sup>3,6</sup> although we will focus on dimeric structures here.

Four hypothetical dinuclear vanadium structures are **6–9**. Structure **6** contains pentacoordinate vanadium and a free hydroxyl arm. The common  $\text{V}_2\text{O}_2$  motif in vanadium(V) complexes is represented by a bridging alkoxide ligand. It is possible that the free hydroxyl arm interacts with another vanadium atom. If this interaction is intramolecular, structure



**7** results. Another related compound with slightly different connectivity is shown in **8**. In both cases the protons are shown on the alkoxide arms, but other possibilities exist and could for

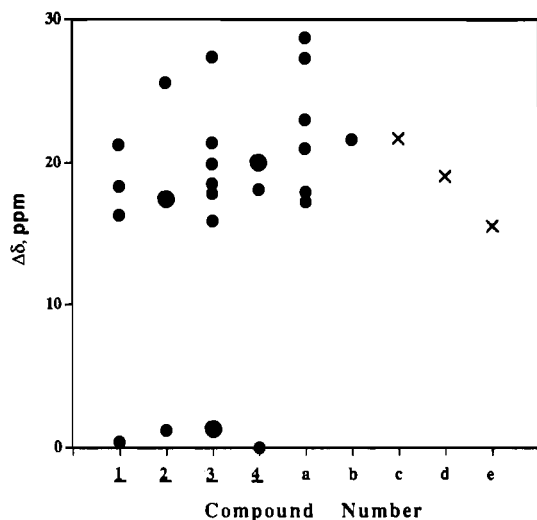


**Figure 12.** Solid-state  $^{13}\text{C}$  NMR  $\Delta\delta$  ( $= \delta_{\alpha\text{-carbon in complex}} - \delta_{\alpha\text{-carbon in free ligand}}$ ) is plotted versus compound number for compounds 1–4 and for  $\text{VO}(\text{OCH}_3)_3$  (a) and  $\text{VO}(\text{OC}(\text{CH}_3)_3)_3$  (b). The solution  $^{13}\text{C}$  NMR  $\Delta\delta$  are shown for  $\text{VO}(\text{OCH}_3)_3$  (c),  $\text{VO}(\text{O-}i\text{-norbornyl})_3$  (d) and  $\text{VO}(\text{OC}(\text{CH}_3)_3)_3$  (e). The  $\Delta\delta$  for each  $\alpha$ -carbon atom in the solid state  $^{13}\text{C}$  NMR spectrum is indicated by ●, if the intensity is twice that of other  $\alpha$ -carbon atoms, it is indicated by ×, the  $\Delta\delta$  for the solution  $^{13}\text{C}$  NMR spectrum for the  $\alpha$ -carbon atom is indicated by ×.

example be distinguished by solid-state  $^{13}\text{C}$  NMR spectroscopy. Dangling alcohol moieties of diols have been described in oxovanadium(V) alkoxide structures.<sup>27</sup> In  $\text{VO}(\text{O-}i\text{-Bu})_2\text{O}(\text{CH}_2)_8\text{-OH}$  one of the two OH groups is dangling presumably due to the length of the methylene chain, which precludes intramolecular association.<sup>27</sup> The entropic term favors interaction with the same vanadium center in compounds 1–4. Structures 7 and 8 are more likely than 6 since solid-state NMR data indicate that the coordination number around the vanadium is six. Lower coordination numbers are not precluded in solution where intermolecular interactions may be weakened.<sup>4a</sup> If both diols interact with the same vanadium and the oxo bridges between the vanadium atoms, structure 9 is obtained. In structure 9, the protons are placed on the bridging oxygen atoms (resulting in bridging OH groups). Other possibilities also exist but are not addressed here. On the basis of the IR bands (see Experimental Section), it appears compounds 1–3 have  $\text{V}=\text{O}$  stretches suggesting that structure 9 is less likely. Compound 4 has a stretch significantly different (at  $950\text{ cm}^{-1}$ ) from the other compounds though it appears to be in the range of  $\text{V}=\text{O}$  stretches. On the basis of the available evidence, compounds 7 and 8 are the two most likely candidates, should these materials be dimeric in the solid state.

Additional structural characterization of compounds 1–4 was achieved by analyzing the solid-state  $^{13}\text{C}$  NMR data. In the case of compound 1, four signals of equal intensity at 97.1, 94.1, 92.1, and 75.5 ppm were obtained for the  $\alpha$ -carbon atoms. This reflects a geometry in which the two *trans*-CHD molecules are asymmetrically coordinated to one vanadium atom; although in a dimeric unit the molecule has some symmetry element. The  $^{13}\text{C}$  NMR data thus favor the connectivity illustrated in 8. We were unsuccessful in producing crystals of compounds 2–4. We were, however, able to grow transparent orange crystals of compound 1 at  $-30\text{ }^\circ\text{C}$  in  $\text{CH}_2\text{Cl}_2$  under a nitrogen atmosphere over several days. Given the fact it was impossible to model the electron density completely due to the presence of disorder in the cyclohexyl rings and alkoxide oxygen atoms, we have chosen not to report

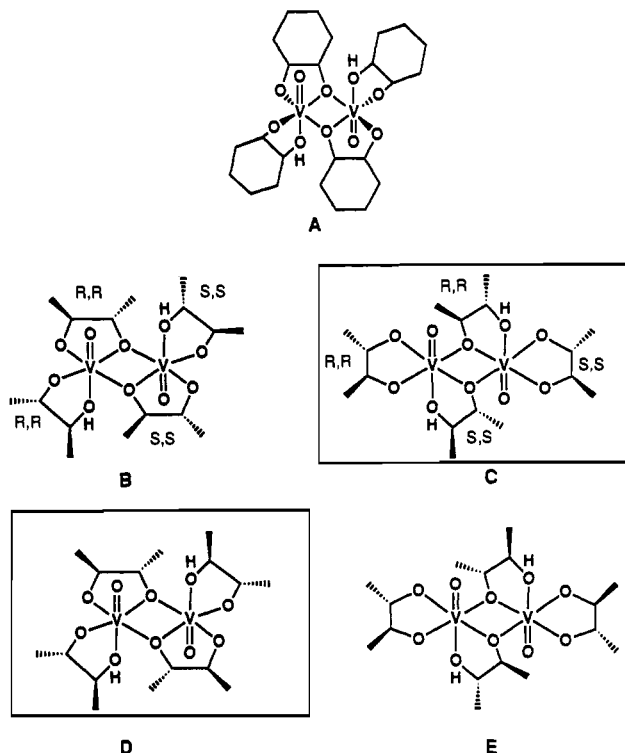


**Figure 13.** Proposed structure for 1 supported by spectroscopic data and limited single-crystal X-ray diffraction (A). Two proposed structures for 2 based on spectroscopic data, a less likely structural analog for this compound (B) and the more likely isomer (C). The proposed structures for 3 (D,E), the more likely (D) and less likely isomers (E).

the coordinates.<sup>28</sup> However, the dimeric structure that was obtained supports the connectivity illustrated in 8 and is shown with *trans*-CHD as the ligand in Figure 13A. The location of the  $\text{H}^+$  shown in these structures were determined by the  $^{13}\text{C}$  NMR chemical shifts. The one  $\alpha$ -carbon bond to an oxygen atom that is weakly interacting with the vanadium (CIS value is close to zero) is most likely in a position *trans* to the terminal oxo group where the weakest of all the  $\text{V}-\text{O}$  interactions should be found. Consequently, we placed the  $\text{H}^+$  as indicated in 8 and Figure 13A.

Consideration of higher oligomers leads to even more complex structures. Available evidence for compound 1 supports a dimeric structure, although higher oligomers could be suggested that would contain this basic dimeric unit. Concentrating on the simplest interpretation of the data, the discussion here will only develop the simplest structural possibilities for compounds 1–4 to satisfactorily explain the observed data.

Analysis of compound 2 (2,3-BD) by solid-state  $^{13}\text{C}$  data shows only three signals representing the four  $\alpha$ -carbon atoms. The higher degree of symmetry would suggest that a structure akin to structure 7 (shown in Figure 13C) is preferred over the structure shown in Figure 13B. Structure C contains two carbon atoms that may very well have similar if not identical chemical shifts.

(28) X-ray data were collected for transparent orange crystals of compound 1 and a partial solution was obtained by direct methods (Miller, M.; Anderson, O. P. Private communication). It was, however, impossible to model the electron density completely, due to the presence of disorder in the cyclohexyl rings and alkoxide oxygen atoms. Given the limitations of this X-ray determination ( $R \sim 0.2$ ), we have chosen not to report the atomic coordinates. However the basic structure appears to be a dimer of the type shown in 8 (see schematics in Figure 13A). Each vanadium atom appears to be bonded to two types of diolate ligands: one in which the diolate oxygen atoms are nonbridging and the second which contains one bridging oxygen atom and one nonbridging diolate oxygen atom. These limited X-ray results are in accord with the information provided by solid-state  $^{51}\text{V}$  and  $^{13}\text{C}$  NMR, elemental analysis, and mass spectroscopy which indicate the structure to be six-coordinate, to have two ligands per vanadium atom and to have a nuclearity greater than one.

The possibilities **6** and **9** were discarded on the basis of the solid-state  $^{51}\text{V}$  NMR evidence favoring an octahedral compound and the IR spectroscopy showing the presence of  $\text{V}=\text{O}$  as described above with compound **1**. Compound **3** (RR-2,3-BD) has a much more complex solid-state  $^{13}\text{C}$  NMR spectrum than compound **2**. There are seven resonances, and the furthest upfield resonance at 73.6 ppm has double the intensity and suggests the presence of two weakly coordinated hydroxyl groups trans to the terminal oxo group. The six other resonances show that none of the other  $\alpha$ -carbons in the dimeric unit are identical, as would be expected since the diol is optically active. Both geometries **7** and **8** could produce the spectrum observed for compound **3**. Given the greater probability of six different resonances for the structure in Figure 13D than that in Figure 13E, the former may be more likely.

The solid-state  $^{13}\text{C}$  NMR spectrum of compound **4** shows three resonances. However, the resonance with the furthest downfield shift represents the  $\alpha$ -carbon with the greatest population in contrast to the spectrum observed for compound **2**. Since large CIS values customarily reflect bridging or formation of a strong bond, this material may not contain a basic structural unit illustrated by **7** and **8** (or **6** and **9**). Since compound **4** is much less soluble than compounds **1**–**3**, this material is distinctly different than the others. Ethylene glycol has previously resulted in formation of an unusual dimeric vanadium complex with the two ethylene glycol units bridging the two vanadium atoms in a 10-membered ring.<sup>4a</sup> Compound **4** may also contain a 10-membered ring in the basic dimeric unit or a new type of bridged structure. Additional bridging or a new type of bridge structure between the dimeric units could increase the coordination number to six (as observed for  $\text{VO}(\text{OCH}_3)_3$ ). We resist further speculation concerning the structure of this material at this time.

In summary, the structural perturbations of the ethylene glycol ligand in comparison to *R,R*-BD and to *trans*-CHD result in oxovanadium(V) complexes with very different structural properties. Although this observation may seem surprising, precedence for structural changes have been reported with ethylene glycol and pinacol in the corresponding oxovanadium(V) chloro alkoxides.<sup>4a,4c</sup> Further exploration of the oxovanadium(V) chloro alkoxide derivatives which are more amenable to characterization by X-ray crystallography, show that significant changes in the

geometry of the complex are observed in the ligand series ethylene glycol, 2,3-butanediol, pinacol, and 1,2-cyclohexanediol.<sup>1a,1c,29</sup> The observations described in this study, despite the lack of satisfactory crystallographic characterization, support similar structural changes in the oxovanadium(V) alkoxides.

### Conclusion

A series of oxovanadium(V) alkoxides with two 1,2-diol ligands per vanadium atom have been synthesized and characterized. These materials associate in solution and undergo ligand exchange. Unfortunately they did not yield crystals of sufficient quality for X-ray characterization. Benchmark data obtained in the present study indicate that solid-state  $^{51}\text{V}$  anisotropic and isotropic chemical shift parameters differentiate between various vanadium(V) coordination environments. The empirical correlation predicts that the new vanadium 1,2-diolate complexes possess distorted octahedral coordination geometries. The results of the present study show that even in the absence of crystallographic information, plausible molecular structures for oxovanadium(V) 1,2-diolates can be deduced on the basis of solution and solid-state NMR studies. The structural differences of the ligands ethylene glycol, 2*R*,3*R*-butanediol, and *trans*-1,2-cyclohexanediol result in oxovanadium(V) complexes with very different geometries and demonstrate the subtle factors affecting the coordination chemistry of such systems.

Given the importance of vanadium-derived intermediates in reactions using vanadium-based catalysts, the studies described here further substantiate the very fine balance between coordination geometries and the respective ligands in vanadium complexes. The simple substitution of a hydrogen atom with a methyl group may affect the preferred coordination geometry both in solution and in the solid state. Information on the governing factors in the coordination preferences of vanadium is therefore desirable before rational design can be employed in further development of vanadium-based heterogeneous and homogeneous catalysts.

**Supplementary Material Available:** Table of IR data (3 pages). Ordering information is given on any current masthead page.

(29) Crans, D. C.; Felty, R. A.; Anderson, O. P.; Miller, M. M. Manuscript in preparation.